

4025

BIOLOGICALLY-INSPIRED HEXAPOD ROBOT DESIGN AND SIMULATION

Kenneth S. Espenschied\*

Roger D. Quinnt†

Department of Mechanical and Aerospace Engineering  
Case Western Reserve University  
Cleveland, Ohio 44106

207627  
P-8

Abstract

The design and construction of a biologically-inspired hexapod robot is presented. A previously developed simulation is modified to include models of the DC drive motors, the motor driver circuits and their transmissions. The application of this simulation to the design and development of the robot is discussed. The mechanisms thought to be responsible for the leg coordination of the walking stick insect were previously applied to control the straight-line locomotion of a robot. We generalized these rules for a robot walking on a plane. This biologically-inspired control strategy is used to control the robot in simulation. Numerical results show that the general body motion and performance of the simulated robot is similar to that of the robot based on our preliminary experimental results.

I. Introduction

This work is part of an interdisciplinary project which aims to develop practical and robust robot control strategies by using principles extracted from neurobiology. In particular, the problem of hexapod robot locomotion is being addressed, and the primary sources of neurobiological data are the American cockroach, the walking stick insect and the locust.<sup>1-4</sup> A simulation was created to aid in the development of a hexapod robot and its controller because of the relative ease of changing parameters and collecting data.<sup>5,6</sup> We have been building robots for the purpose of further developing, testing, and demonstrating these controllers.

Walking robots have been of interest throughout the history of robotics, including numerous examples with one, two, four and six legs.<sup>7-16</sup> Hexapods are particularly common because they can reposition half of their legs while supporting the body in a statically stable fashion with the other half. With six legs, however, many actuators are required and weight becomes a major design concern. Thus, some method of simplifying the locomotion is often applied, such as the use of pantograph mechanisms which decouple the horizontal and vertical motion.<sup>15,17</sup>

Despite steady progress in the field of robotics, today's walking robots have limited locomotion capabilities compared to insects, which execute this complex task with remarkable skill and robustness. Researchers are making use of biological principles to design robots and their controllers. For example, Raibert has constructed a variety of successful hopping robots controlled based on the principle of the inverse pendulum as in human running.<sup>7,8</sup>

From neurobiology, it is known that there is a close link between the nervous system and the physiology of any animal. In attempting to create a system which achieves successful locomotion by incorporating strategies from the insect world, it may be desirable to start with an insect-like robot.

Hence, there is an interest in building biologically-inspired robots and exploiting the synergies found in insects between their mechanics and their control systems. For example, Donner employed a biologically-inspired approach for gait generation in a hexapod robot.<sup>18</sup> Brooks and Ferrell have built small hexapod robots and controlled them using finite state algorithms.<sup>16,19</sup>

Previously, a small hexapod was built and its straight-line locomotion on a flat surface was controlled using a biologically-inspired neural network.<sup>20</sup> The purpose of the robot was to test the controller which was previously developed and demonstrated using a kinematic simulation.<sup>21</sup> This neural network was shown to be robust to the severing of any central or sensory connection.<sup>22</sup> It produced a continuum of statically stable insect-like gaits as a single scalar input governing the speed of the robot was varied.<sup>20</sup> Three mechanisms thought to be responsible for coordination in the walking stick insect were applied to the same locomotion task.<sup>23</sup>

The robot discussed in this paper is more insect-like than the previous robot in terms of leg configuration and degrees of freedom. It is designed to be capable of turning, walking on a rough terrain and walking quickly which requires careful consideration of power and weight. Animal muscle has a high power to weight ratio and controllability that is difficult to reproduce with present technology. The power to weight ratio of DC motors is much less than that of insect muscle. Despite this, DC motors are typically used in robotics because of their controllability.

Every item on a legged robot contributes to the total weight that its legs must lift. It is typical for one leg to support half of the body weight, and in this case, an individual motor may have to support its entire load. A motor which is lightly loaded in one configuration may be heavily loaded in a different configuration, thus, for a highly mobile robot, whose legs may undergo many different configurations, many of the motors must be equally powerful.

In this paper, a previous simulation is reviewed which was developed to assist in the design of the robot, and in particular to help choose appropriate motors and transmissions.<sup>5,6</sup> Next, the design and construction of the robot are discussed. Then, modifications to the previous simulation are introduced to more accurately model the dynamics of the robot. A biologically-inspired controller based on the mechanisms which coordinate the legs of the stick insect is then reviewed. Next, this controller is modified and generalized for the control of the robot walking on a plane. Numerical results demonstrate the locomotion of the simulated hexapod using this controller. The general body motion and performance of the simulated robot are similar to that of the robot based on our preliminary experimental results.

\* Research Associate

† Associate Professor, Member AIAA

## II. Review of A Simplified Dynamic Model of a Hexapod Robot

Lin and Quinn developed equations which describe the motion of an insect-like walking robot.<sup>5,6</sup> The robot was modeled as having a central body and six legs, each leg having two segments and three revolute degrees of freedom, two where the leg joins the body (hip) and one connecting the two segments (knee). They formulated a simplified dynamic model based on the assumption that the inertia of each leg is much less than the inertia of the central body. This is the case for most insects (for example, all six legs account for approximately 12% of the total mass of a cockroach).

The assumption that the inertia of the leg is much smaller than the inertia of the central body leads to the following conclusions:

(i) Each leg which is in its power stroke (stance) may be treated as if it is in static equilibrium and kinematic equations govern its motion.

(ii) The reactions acting on the body at the hip joint of a leg which is in its recovery stroke (swing) are much less than the reactions at the hip joint of a leg in stance and, therefore, can be neglected.

Hence, the forces and moments at the hips acting on the central body are assumed to be due to the stance legs only. Also, given the joint torques, these forces and moments can be determined approximately based on static equilibrium using the Jacobian matrix of each stance leg.

The central body is treated as rigid with six degrees of freedom. Each stance leg is treated as a manipulator pivoted at the ground contact point with the body treated as its end-effector. On the other hand, a leg in the return stroke is treated as a manipulator with a moving base (the hip). Hence, the equations of motion are decoupled into dynamic equations for the central body, dynamic equations for each leg which is in the recovery phase, and kinematic equations to represent each leg which is in the stance phase. In comparison with the full dynamic model, the number of equations are the same, but, in the simplified model, the equations are decoupled into a set of less complex systems. Because the equations are decoupled, the leg masses are included in the swinging leg equations as well as in the mass of the body. The leg masses are counted as point masses at their respective hip joints, thus the central body mass is set to the mass of the entire robot. This assumption is justified because the motors, which comprise most of the mass, are located near the hip on the robot described in the next section.

During each time step the simulation is set up as an initial value problem, and given the joint torques, the Newton-Euler equations governing the motion of the central body are integrated to determine the state of the body at the next time step. Then, the equations governing the motion of each leg are integrated to determine its state at that time step. If a leg in its stance phase is found to be in tension, it is switched to the recovery phase. Alternately, when the foot of a swinging leg is found to contact the ground, that leg is switched to the stance phase.

Note that, because the inertia of a stance leg is neglected, the constraint force caused by the ground acting on the foot and the joint forces at the knee joint and at the hip joint are equivalent. Hence, the ground reactions at the foot can be determined from knowledge of the joint torques and will not be unknowns in the simulation problem.

In the simulation, the joint torques and the ground reactions are unknown and are to be determined for a particular walking gait and corresponding joint

motions. In general, given a dynamic model of a walking system, when more than one foot is in contact with the ground, a closed kinematic chain is formed and there are an infinite number of solutions to the problem. Pfeiffer et al. used an optimization technique to choose a particular set of feedforward control joint torques.<sup>24</sup> On the other hand, Quinn and Lin used a feedback control strategy to determine the required joint torques to cause the joints to follow the desired joint motions. Both of these strategies have a basis in biology. Lin and Quinn used collocated, proportional-derivative (PD) feedback control which effectively provided active springs and dampers at the joints. The active stiffness and damping gains were chosen to be proportional to the inertia of the link they control. At each time step, the joint torques were determined as proportional to the error between the actual joint motion and the desired joint motion. The ground reactions were then determined using the simplified dynamic model and the equations of motion were integrated as discussed above.

Simulations were performed in which the robot was desired to walk at a constant speed along a straight-line along a smooth horizontal surface. The desired motions of the simulated robot's joints were determined based on metachronal (rear-to-front stepping sequence) insect-like walking gaits. The results showed that each pair of legs displayed a unique insect-like ground reaction force pattern.

## III. Design and Construction of a Hexapod Robot

The robot and controller system consists of a personal computer, 18 motor controller circuits contained in a motor controller box, and the robot itself. The computer is connected to the motor controller box with a digital bus, which in turn is connected to the robot by an electrical tether.

The robot, shown in Fig. 1, has a mass of about 5 kg, and is about 50 cm long, 30cm high, and 36cm wide with its legs retracted. The length of an extended leg is about 50cm, and the foot-to-foot distance of opposite, extended legs is about 1.1m. Each leg has three segments, a coxa, a femur, and a tibia, as they are referred to in the insect. The coxa is connected to the body via a revolute joint with its axis perpendicular to the plane of the body (joint 1). The femur attaches to the coxa with a revolute joint with its axis parallel to the body plane (joint 2). Also, the revolute joint connecting the femur and tibia is parallel to the plane of the body (joint 3). Thus, there are three active (motor-driven) joints per leg. In addition, the tibia has a spring loaded linear bearing so that it may compress passively in the axial



Fig. 1. Photograph of the robot.

direction, thus adding a fourth, passive degree of freedom to each leg. The purpose of this degree-of-freedom is to mechanically store energy to augment the actuators, and to reduce impact forces which are generated when a foot contacts the ground. R. McN. Alexander emphasizes the importance of elastic elements in the locomotion of animals, and encourages their application in robotics.<sup>25</sup> We have attempted to incorporate springs in our robot to gain some of the advantages enjoyed by animals.

The robot is constructed mostly of aircraft plywood and balsa wood to minimize mass and inertia. The femurs, which are mostly balsa, are coated with mylar to increase surface toughness. The long, slender section of the tibia is aluminum tube with a rubber tip for a foot. Joint components are mostly aluminum because they are subjected to relatively high stresses. However, the axles for the hip's vertical axis are stainless steel. The attachment between this axle and the body is reinforced with carbon and kevlar fibers. All the joints are supported by ball bearings.

Each of the 18 active joints is driven with a 6 Watt DC motor with an attached planetary transmission. The motors are located near the hip to reduce the inertia of the leg. Joint positions are sensed with potentiometers, and the axial load in each tibia is sensed by a pair of semiconductor strain gages.

To supply an input to the motor, there are digital circuits which make use of pulse-width modulation to control the motor output. The motor controller circuit contains an EPROM so that the control law may be easily modified. Each circuit contains two analog to digital converters. One of these directly converts an analog signal, and this is used for the position feedback. The other one is coupled to a 10x gain to amplify the input voltage before it is converted to digital. This channel was designed for use with the semiconductor strain gages measuring the axial force in the tibia. Also, the joint torque may be estimated by monitoring the output of the motor controller circuits.

#### IV. Modifications to the Previous Simulation

The net transmission efficiency under the typical operating conditions of the robot was measured to be about 40%. This relatively poor performance is due to the large torques that they transmit to lift the body. Clearly the transmission efficiency plays a major role in the system, contributing to large power losses and reducing backdrivability. Therefore, an adequate simulation of the robot must include a transmission model which reflects this.

Transmission efficiency is related to the load dependent, Coulomb frictional force that results as gear teeth slide upon one another. In developing a transmission model of this phenomenon the difficult problem of modeling a statically indeterminate system is encountered. For example, in the simplest model that includes transmission efficiency, the motor output is multiplied by the efficiency when the motor is doing positive work (driving the joint) and divided by the efficiency when the motor is doing negative work (being backdriven by the joint). In this model a discontinuity occurs when the motor speed changes direction. In fact, the joint torque suddenly changes by a factor of about 5 with 40% transmission efficiency when the speed changes sign. Thus, there is a great potential for instability in this most simple model because of this discontinuity in torque.

Because of the complexity of implementing a truly rigorous transmission model, the simplified model shown in Fig. 2 was developed to represent the frictional characteristics of the transmission. The

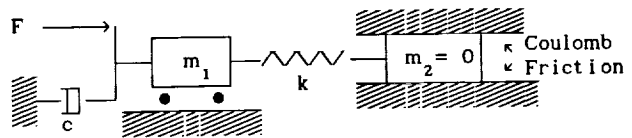


Figure 2. Schematic of motor and transmission model.  $m_1$  represents the inertia of the joint.  $F$  is the motor torque.  $c$  is a viscous damping constant measured from the motor torque/speed characteristics and  $k$  is a stiffness constant. The block on the right is modeled with no inertia and slides on a rough surface subject to Coulomb friction. The maximum magnitude of the Coulomb friction is a function of the motor torque.

purpose of this model is to smooth the above noted discontinuity yet maintain simplicity to permit a straightforward implementation. To account for the torque loss due to transmission inefficiency, a massless auxiliary body was envisioned as added to each joint. This body is coupled to the motion of the joint via a stiff spring. Since the body is massless, the force in the spring is determined only by the frictional force between the body and ground (the stationary side of the joint). The maximum frictional force is limited by the torque output and direction of motion of the motor. Depending upon the sign of the work performed by the motor, the transmission output is described as follows:

$$\tau_{out} = \tau_{mot} + \tau_{loss} \quad (1)$$

where, when the motor is doing positive work, the torque loss is

$$\tau_{loss} = \tau_{mot} (e - 1) \quad (2)$$

and when the motor is doing negative work, the torque loss is

$$\tau_{loss} = \tau_{mot} \left[ \frac{1}{e} - 1 \right] \quad (3)$$

where  $\tau_{mot}$ ,  $e$  and  $\tau_{loss}$  are the motor torque (the output of the motor multiplied by the transmission ratio), transmission efficiency and torque loss in the transmission due to inefficiency, respectively.

The magnitude of the torque that the spring can apply to the joint is limited to the magnitude of the frictional loss in the transmission by adjusting the position of the auxiliary body. Care is taken not to change the direction of the spring compression when the body slips, as this also would cause a relatively large discontinuity. When the spring is compressed and the auxiliary body is moving with the joint in one direction, then the inefficiency is being modeled accurately. If the velocity then reverses, the spring will decompress as the joint begins to move in the other direction. Eventually, it stretches, and, when the tension in the spring reaches the limit, the auxiliary body begins to slide and accurately model transmission inefficiency again.

This model of transmission inefficiency works best on joints which undergo relatively large motions instead of joints which have high load and maintain nearly constant position over time. The reason is that the spring may store some energy and actually help the motor when the real frictional force would hinder the motor. This effect is minimized by using a stiff spring. However, as the stiffness approaches infinity, the output torque approaches the discontinuity discussed above and instability is imminent. We can determine which joints are

effectively modeled by this method from the joint torque, motor torque, and joint velocity data, and interpret the results accordingly. The model may be more useful on undulating terrain than on perfectly flat terrain because the joints will tend to undergo larger motions in this case.

The inertias of the motor rotors were neglected. The reflected value of the rotor inertia is about 40% less than the inertia of the lightest leg segment, the tibia. The loads on this joint when the leg is in the air are very low, and are not of considerable interest.

New graphical output was added to the simulation, along with new code to play back the graphical data files in real time. The previous simulation contained graphic capability, but it was not compatible with the present machine that is running the simulation. The graphical output is of great value in quickly evaluating whether the simulation output is realistic or not, and how natural it appears.

#### V. Review of Previous Locomotion Controller

As a first step at using a biologically-inspired controller for the locomotion of the simulated hexapod, a generalization of a previous biologically-inspired controller was used. Before describing the modifications, we will first review the operation of the previous controller.<sup>23</sup>

Cruise reviewed three of the mechanisms thought to be responsible for the leg coordination of the stick insect.<sup>3</sup> Dean further describes these mechanisms and shows excellent results for generating insect-like gaits for straight-line locomotion in kinematic simulations.<sup>26,27</sup> In this model of coordination, the insect leg moves between two positions, the Posterior Extreme Position (PEP), and the Anterior Extreme Position (AEP), which are both scalars measured in the body reference frame, where positive is defined as forward. When the leg supports the body and propels the body forward, the foot approaches the PEP. When it reaches the PEP, the foot lifts and moves forward toward the AEP. When it reaches the AEP, the foot is planted and the leg begins to propel the body again. The coordinating influences shift the PEP and AEP from their intrinsic positions, iPEP and iAEP, respectively, and thus phase-shift the stepping cycle of the legs to coordinate them.

Three of these mechanisms were previously applied to the task of straight-line locomotion on a flat surface for a twelve degree of freedom hexapod robot.<sup>23</sup> In this implementation, the coordination mechanisms used only effect the PEP. The mechanisms work to adjust the PEP's in the following way:

1. Each leg produces mechanism outputs unique to that leg. Three mechanisms were used, so there are three mechanism outputs for each leg. The mechanism outputs are plotted in the top three graphs of Fig. 3. These outputs are a function of time and the foot position. The foot position is shown in the lower graph of the same figure.

2. An influence is a dedicated channel through which one mechanism of one particular leg (sending leg) can affect the PEP of another leg (receiving leg). Note that the terms "sending leg" and "receiving leg" are relative only to the influence being discussed. Each influence consists of a weight times the output of the specified mechanism of the sending leg. There is a total of 26 influences in our implementation, all of which have positive weights. Figure 4 illustrates these influences. Each arrow is an individual influence, and the number in the arrow indicates the mechanism that the influence weight multiplies.

3. For each leg, the PEP is adjusted from the iPEP position by an amount equal to the sum of all influences converging on that leg. Notice in Fig. 3 that the position of the foot decreases until it intersects the PEP trace, then it begins to increase. Note, however, that the PEP is adjusted based on influences from mechanism outputs of other legs, not from the mechanism outputs shown in the same figure. The AEP, which is not shown, is a constant, and that is why the position trace always peaks at the same level.

The result of applying this control strategy to the previous robot was a continuous range of statically-stable insect-like gaits, from the slow, metachronal wave (back-middle-front stepping sequence) to the relatively fast tripod gait (middle leg on one

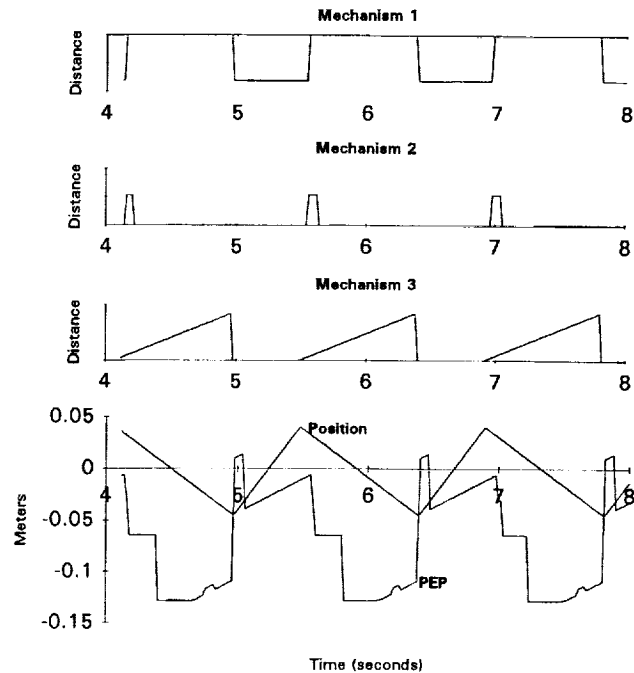


Fig. 3. Leg coordination mechanisms.

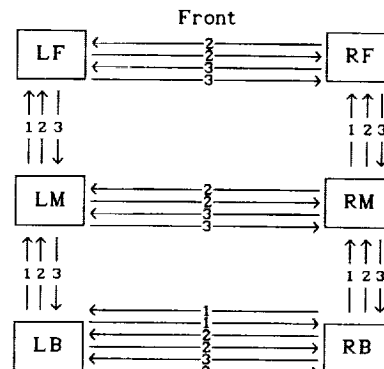


Figure 4. Influences. Each box indicates a leg. L, R, F, M, and B, denote left, right, front, middle, and back, respectively. Each influence is shown by an arrow. The number in the arrow indicates the mechanism to which the influence is proportional.

side of the body steps in unison with the front and back legs on the other side, while each left leg steps in antiphase with the corresponding right leg). There was a single scalar input governing the speed of locomotion, but the resulting gait was produced by the dynamic interaction within the controller and was not pre-programmed. The controller was found to be robust in the sense that it was insensitive to changes in most parameters.

#### VI. Modifications to the Controller

The new strategy generalizes these rules to locomotion on a plane. The inputs to the controller are forward body velocity, lateral body velocity, and angular rate of body rotation about the vertical axis (yaw rate). The modified controller generates the same range of gaits for forward locomotion, but with the additional ability to "crab" laterally and yaw.

These rules were generalized with the creation of a 1-dimensional variable which is a measurement of the displacement of the current desired foot position from the center of the leg's workspace (home position), in the direction opposite the current foot motion relative to the body. This distance is computed by

$$x = - \frac{\vec{x}_{fh} \cdot \vec{v}_d}{|\vec{v}_d|} \quad (4)$$

where  $\vec{x}_{fh}$  is the vector from the home position to the current desired foot position, and  $\vec{v}_d$  is the current desired velocity of the foot relative to the body. The variable  $x$  corresponds to the position trace in the lower graph of Fig. 3, and is used to compute new mechanism outputs for each leg, then compared to the PEP and the AEP to determine whether the leg should change states (from power to return stroke or vice-versa).

When the leg is in the power stroke, the desired velocity  $\vec{v}_d$  is computed at each time step. During the return stroke, however,  $\vec{v}_d$  is not calculated. When the leg transitions from power to return stroke, a desired velocity  $\vec{v}_{dup}$  is computed such that the leg will remain up for a fixed time, and during this time the desired position will move from its present location to where a vector in the direction of  $-\vec{v}_d$  starting at the home position would intersect a circle of radius AEP centered about the home position. Thus, if the desired body motion reverses while a leg is in the return stroke, then it continues its present course until it switches to power stroke, at which time it may begin a new return stroke in the appropriate direction. This approach simplifies the return stroke.

The desired velocity  $\vec{v}_d$  of the foot relative to the body is computed from the desired forward, lateral, and yaw rates of the body in combination with the current desired foot position. Thus, the feet can each have a different desired foot velocity.

The desired vertical coordinate of the foot relative to the body is adjusted based on whether the leg is in the return or power stroke. If the leg is in the return stroke, the desired vertical component is incremented a fixed amount per time step until it reaches the desired maximum, and if the leg is in the power stroke, the desired vertical component is decremented until it reaches the desired minimum.

#### VII. Numerical Results

The masses, inertias and link length parameters in the simulation were set to correspond to those of the robot. By experimentation we approximated the effective stiffnesses of the robot's joints. For the simulation, we chose the gains for the proportional controller so that the effective stiffnesses of the joints of the simulated robot closely matched those of the robot.

In the previous dynamic simulation, PD control was used.<sup>5,6</sup> The motor model, however, includes viscous damping due to the back emf generated by the motor. Therefore, in the simulation results presented here, we used proportional control only. The motors provide sufficient damping to maintain stability. This was also found to be true for the robot. In the insect, it appears that viscous forces are significant, based on preliminary results from.<sup>28</sup>

The midrange, no-load configuration of the simulated robot is such that the femurs are extended laterally and inclined approximately 45 degrees from the horizontal and the tibias are vertical. Figure 5 shows the graphical output which was added to the previous simulation. The simulated robot is shown as a stick-figure casting a shadow on the plane below it. Note that the simulated robot is under load and walking and, thus, the joints are deflected.

The generalized control scheme described above was interfaced with the modified dynamic model of the robot. The simulated robot successfully walks on a smooth level surface in a continuum of statically stable gaits in response to three inputs: forward velocity, lateral velocity and yaw rate. The general body motion and performance are similar to that of the robot based on our preliminary experimental results. In the simulations, the controller typically causes the simulated robot to settle into a regular gait in just a few steps.

Footfall data illustrating the range of gaits is presented in Fig. 6. Each leg has a trace which is plotted against time, and the trace is only visible when the leg is in the return stroke. These footfall patterns illustrate two features of this controller: The range of gaits that it can produce and the speed with which it settles into these gaits. The top portion of the figure shows the tripod gait and the lower portion shows a slower metachronal wave gait. The middle plot is a medium speed gait. Figure 7 shows the body roll and pitch during the tripod gait shown in Fig. 6.

Because the particular influences chosen were based on forward walking of the stick insect, during sideways or even backwards stepping the gait is still a back-middle-front metachronal wave. In future work we may adjust these influences based on the desired direction of motion. We would like to emphasize that the sideways and backwards gaits are statically

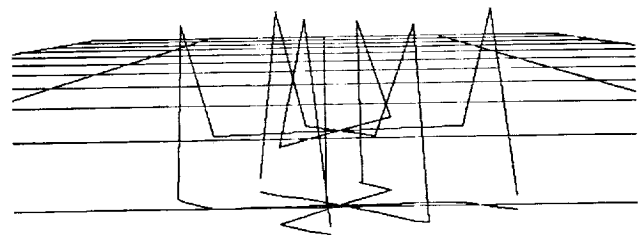


Fig. 5. Simulation environment.

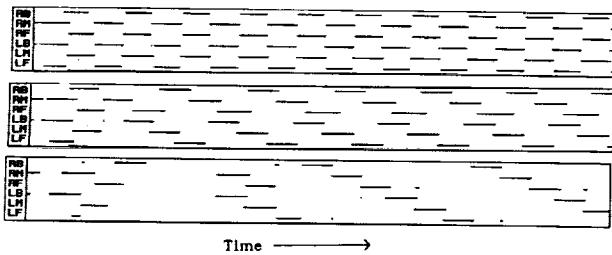


Fig. 6. Stepping patterns for several gaits.

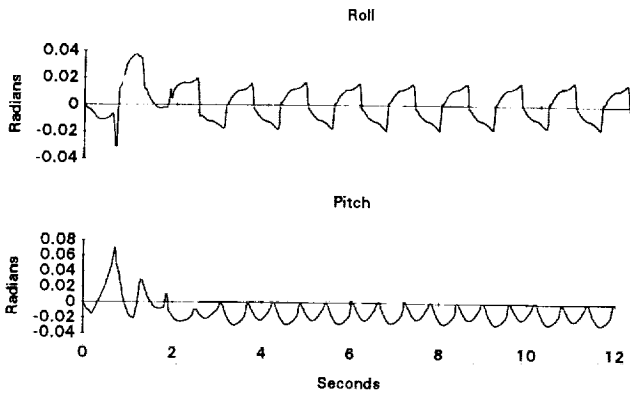


Fig. 7. Roll and Pitch of body during tripod gait.

stable, but not necessarily insect-like nor optimal for static stability. The controller does sometimes try to lift two adjacent legs when the inputs are changed quickly, but it does adequately maintain static stability when the input is changed gradually, and allows for a wide range of walking behavior.

Figure 8 displays the ground reaction forces for the three left legs while the simulated robot walks in the medium speed gait shown in Fig. 6. In these figures, the X direction is forward, Y points to the left, and Z is upward relative to the body. Note that while the simulated robot is walking at a steady average speed, the front legs tend to decelerate the body, the rear legs tend to accelerate the body, and the middle legs first decelerate then accelerate the body during their respective drive phases. The lateral (Y) forces are directed toward the body for all legs. Similar force patterns have been observed for insect locomotion.<sup>2</sup> The previous simulation, in which PD control was used, also exhibited this insect-like force pattern.<sup>5,6</sup> However, the effect in the X direction was more pronounced than in this modified simulation. Figure 9 shows the ground reaction forces in the X direction for the left rear leg using a transmission efficiency of 40% and 100%. This effect is more pronounced in the 100% efficiency case. We conclude from this that Coulomb friction is responsible for this difference.

Figure 10 shows the position versus time for joint 2 (front to back swing) of the left middle leg, which corresponds to the medium speed gait shown in Fig. 6. The function of the transmission model (see Fig. 2) is illustrated in Fig. 11 which shows motor torque (multiplied by transmission ratio) and total joint torque vs. time for joint 2 (front to back

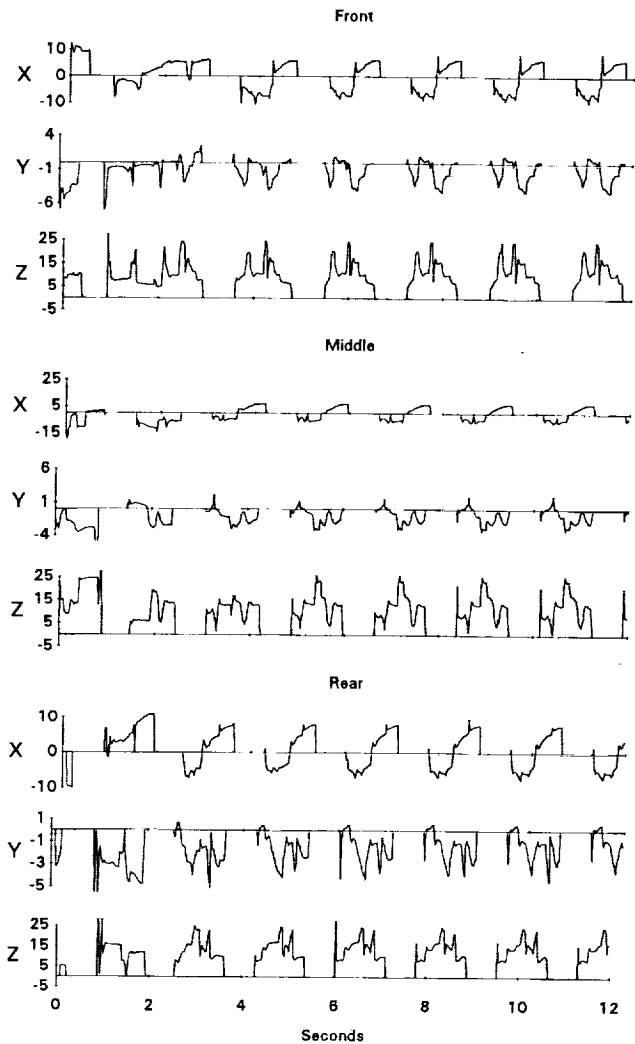


Fig. 8. Ground Reaction forces for left legs.

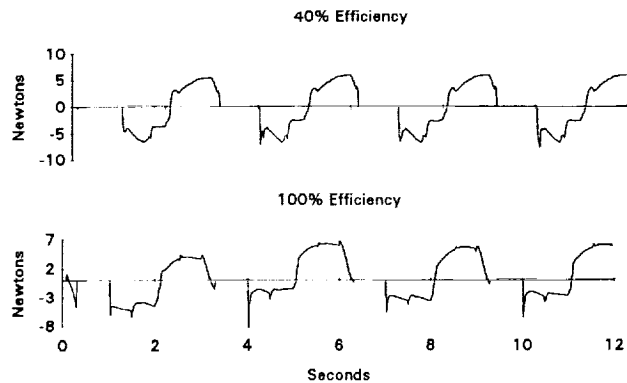


Fig. 9. Effect of transmission efficiency on x ground reactions (LR leg).

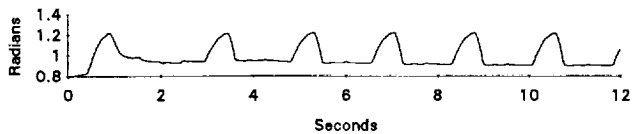


Fig. 10. Joint 2 position vs. time (LM leg).

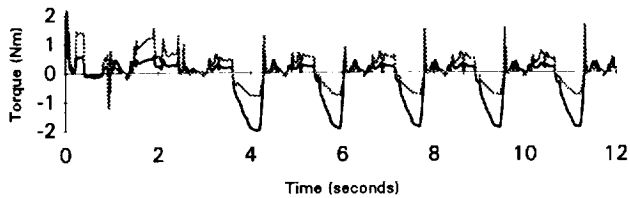


Fig. 11. Motor and joint 1 torque vs. time (LM leg).

swing) for the left middle leg. Note that when the leg is in the recovery stroke the motor is doing positive work and its torque is higher than the joint torque. In the first half of the power stroke, the motor does negative work (slows the body), and in the second half it does positive work (propels the body). Notice that the magnitude of the motor torque is less than the joint torque during the negative work phase (when torque is negative in this case) and greater than the joint torque when the work is positive (positive torque in this case) as one would expect from transmission inefficiency.

#### VIII. Summary

The design and construction of a small 18 degree of freedom robot is described. The robot is designed to walk on rough terrain. We modified a previous simulation of an 18 degree of freedom hexapod to increase its utility for the task of design and modeling of a hexapod robot. The most significant modifications were to add models of the motor driver circuit, motor, and transmission, including a simplified model of transmission inefficiency. A previously designed biologically-inspired locomotion controller, which originally produced straight-line forward locomotion on a flat surface, was generalized to produce lateral and turning motion. This generalized control scheme was interfaced with the modified dynamic model of the robot. The simulated robot successfully walks on a smooth level surface in a continuum of statically stable gaits in response to three inputs: forward velocity, lateral velocity and yaw rate. The general body motion and performance are similar to that of the robot based on our preliminary experimental results. In the simulations, the controller typically causes the simulated robot to settle into a regular gait in just a few steps. The ground reaction forces generated by the locomotion share significant features with force data on insect locomotion.

#### Acknowledgements

We would like to thank Harold P. Frisch of the NASA Goddard Space Flight Center for grant NGT-50588 and Dr. Thomas McKenna of the Office of Naval Research for grant N00014-90-J-1545. The Cleveland Advanced Manufacturing Program supplied additional funding through the Center for Automation and Intelligent Systems Research at CWRU.

#### IX. References

1. Ritzmann, R. E., "The neural organization of the cockroach escape and its role in context dependent orientation," In R. D. Beer, R. E. Ritzmann, and T. McKenna (Eds.), *Biological neural networks in invertebrate neuroethology and robotics*. New York: Academic Press, 1992.
2. Full, R. J., Blickhan, R., and Ting, L. H., "Leg design in hexapedal runners," *Journal of Experimental Biology*, 158, 369-390, 1991.
3. Cruse, H., "What mechanisms coordinate leg movement in walking arthropods?" *Trends in Neural Science*, 13, 15-21, 1990.
4. Pearson, K. G., and Franklin, R., "Characteristics of leg movements and patterns of coordination in locusts walking on rough terrain," *The International Journal of Robotics Research*, 3(2), 101-112, 1984.
5. Lin, N.J., "Dynamics and Control of Open- and Closed-Chained Multibody Systems," Ph.D. Dissertation, Case Western Reserve University, 1992.
6. Quinn, R. D. and Lin, N. J., "Dynamics and Simulation of an Insect-Like Walking Robot," Proceedings of the Ninth VPI&SU Symposium on Dynamics and Control of Large Structures, May 10-12, 1993
7. Raibert, M.H., *Legged Robots that Balance*. Cambridge, MA: The MIT Press, 1986.
8. Hodgins, J.K. and Raibert, M.H., "Adjusting step length for rough terrain locomotion," *IEEE Transactions on Robotics and Automation*, 7, 289-298, 1991.
9. Miura, H. and Shimoyama, I., "Dynamic walk of a biped," *The International Journal of Robotics Research*, 3, 60-74, 1984.
10. Liston, R.A. and Mosher, R.S., "A versatile walking truck," *Proceedings of the 1968 Transportation Engineering Conference*, ASME-NYAS, Washington, D.C, 1968.
11. Raibert, M.H., Chepponis, M., Brown, H.B. Jr., "Running on four legs as though they were one," *IEEE Journal of Robotics and Automation*, RA-2, 70-82, 1986.
12. Hirose, S. and Kunieda, O., "Generalized standard foot trajectory for a quadruped walking vehicle," *The International Journal of Robotics Research*, 10, 3-12, 1991.
13. McGhee, R.B., "Vehicular legged locomotion." In G.N. Saridis (Ed.), *Advances in Automation and Robotics*. JAI Press, 1983.
14. Byrd, J.S. and DeVries, K.R., "A six-legged telerobot for nuclear applications development," *International Journal of Robotics Research*, 9, 43-52, 1990.
15. Song, S. M. and Waldron, K. J., *Machines that walk*. Cambridge, MA: The MIT Press, 1989.
16. Brooks, R.A., "A robot that walks; emergent behaviors from a carefully evolved network," *Neural Computation*, 1, 253-262, 1989.
17. Hirose, S., "A study of design and control of a quadruped walking vehicle," *The International Journal of Robotics Research*, 3, 113-33, 1984.
18. Donner, M.D., *Real Time Control of Walking*. Boston: Birkhäuser, 1987.
19. Ferrell, C., "Robust Agent Control of an Autonomous Robot with Many Sensors and Actuators," Ph.D. Dissertation, M.I.T., May 1993.
20. Quinn, R.D. and Espenschied, K.S., "Control of a hexapod robot using a biologically inspired neural network," In R.D. Beer, R.E. Ritzmann, and T. McKenna (Eds.), *Biological Neural Networks in Invertebrate Neuroethology and Robotics* (pp. 365-381). New York: Academic Press, 1992.

21. Beer, R. D., and Chiel, H. J., "Simulations of cockroach locomotion and escape," In R. D. Beer, R. E. Ritzmann, and T. McKenna (Eds.), *Biological neural networks in invertebrate neuroethology and robotics*. New York: Academic Press, 1992.
22. Chiel, H. J., Beer, R. D., Quinn, R. D., and Espenschied, K. S., "Robustness of a distributed neural network controller for locomotion in a hexapod robot," *IEEE Transactions on Robotics and Automation*, 8, 293-303, 1992.
23. Espenschied, K. S., Quinn, R. D., Chiel, H. J., and Beer, R. D., "Leg coordination mechanisms in the Stick Insect Applied to Hexapod Robot Locomotion," *Adaptive Behavior*, 1(4), 455-468, 1993.
24. Pfeiffer, F., Weidemann, H. J., and Danowski, P., "Dynamics of the Walking Stick Insect," *IEEE Control Systems*, pp. 9-13, February 1991.
25. Alexander, R. McN., "Three uses for springs in legged locomotion," *The International Journal of Robotics Research*, 9(2), 53-61, 1990.
26. Dean, J., "A model of leg coordination in the stick insect, *Carausius morosus*; III. Responses to perturbations of normal coordination," *Biological Cybernetics*, 66, 335-343, 1992.
27. Dean, J., "A model of leg coordination in the stick insect, *Carausius morosus*; IV. Comparisons of different forms of coordinating mechanisms," *Biological Cybernetics*, 66, 345-355, 1992.
28. Marx, W. J., Beer, R. D., Nelson, G. M., Quinn, R. D., and Crocker, G. A., "A Biomechanical Model of the Cockroach," presented at the Annual Meeting of the Society for Neuroscience, Washington, D.C., Nov. 7-12, 1993.